Journal of Biomolecular NMR (2005) 32: 195–207
DOI 10.1007/s10858-005-8073-y

Article

Water–protein hydrogen exchange in the micro-crystalline protein Crh as observed by solid state NMR spectroscopy

Anja Böckmann[a,*], Michel Juy[a], Emmanuel Bettler[a], Lyndon Emsley[b], Anne Galinier[c], François Penin[a] & Anne Lesage[b,*]

[a]*IFR 128 BioSciences Lyon-Gerland, Institut de Biologie et Chimie des Protéines UMR 5086 CNRS/ULCB, 7, passage du Vercors, 69367, Lyon France;* [b]*Laboratoire de Chimie, UMR 5182 CNRS/ENS, Ecole Normale Supérieure de Lyon, 46 Allee d'Italie, 69364, Lyon France;* [c]*Institut de Biologie Structurale et Microbiologie, 31 chemin Joseph Aiguier, 13402, Marseille France*

Received 4 February 2005; Accepted 19 May 2005

Key words: hydrogen exchange, magic angle spinning, micro-crystalline, protein, solid-state NMR, water

Abstract

We report site-resolved observation of hydrogen exchange in the micro-crystalline protein Crh. Our approach is based on the use of proton T_2' -selective ^1H–^{13}C–^{13}C correlation spectra for site-specific assignments of carbons nearby labile protein protons. We compare the proton T_2' selective scheme to frequency selective water observation in deuterated proteins, and discuss the impacts of deuteration on ^{13}C linewidths in Crh. We observe that in micro-crystalline proteins, solvent accessible hydroxyl and amino protons show comparable exchange rates with water protons as for proteins in solution, and that structural constraints, such as hydrogen bonding or solvent accessibility, more significantly reduce exchange rates.

Abbreviations: SSNMR – solid state NMR; MAS – magic angle spinning; Crh – catabolite repression histidine-containing phosphocarrier protein; HPr – histidine-containing phosphocarrier protein; MRI – magnetic resonance imaging; PEG – polyethylene glycol; DSS – 2,2-dimethylsilapentane-5-sulfonic acid; CP – cross polarization; PDSD – proton driven spin diffusion

Introduction

The hydration of a protein, involving the structure and dynamics of surrounding water, is important to such key features as the stability and the folding (or misfolding) of the protein. Notably, hydrogen exchange between protein protons and water protons has been shown to be an indicator for solvent accessibility, and the implication of protein protons in hydrogen bonds, and thus yields valuable structural and dynamical information of the protein. For proteins in solution, the analysis of slow hydrogen exchange, as observed by $^1H/^2H$ chemical exchange, allows a wide variety of studies, including protein folding (see for example Buck et al., 1994; Raschke and Marqusee, 1998; Krishna et al., 2004). Magnetization transfer techniques have been successfully applied to study fast exchange processes between solvent water and exchangeable sites in biomolecules (Dobson et al., 1986; Spera et al., 1991; Liepinsh et al., 1992; Böckmann et al., 1996; Mori et al., 1996; Hwang et al., 1998; Böckmann and Guittet, 1997). Water–protein chemical exchange has also been extensively studied *in vitro*

*To whom correspondence should be addressed. E-mail: a.bockmann@ibcp.fr; anne.lesage@ens-lyon.fr

and *in vivo* (see for example van Zijl et al., 2003) in regard to its importance in magnetization transfer processes in magnetic resonance imaging (MRI) (Liepinsh and Otting, 1996).

Few studies, however, exist on hydrogen exchange in solid proteins. Early work from Harbison et al. reports fast exchange of Lysine εNH_3^+ protons in Bacteriorhodopsin (Harbison et al., 1988). Dobson and coworkers analyzed slow hydrogen exchange in crystals of lyzsozyme (Bentley et al., 1983; Pedersen et al., 1991); a similar study was conducted by Woodward and coworkers in BPTI (Gallagher et al., 1992). ^2H magnetic relaxation dispersion in crystalline BPTI showed the dominant contribution of rapidly exchanging deuterons to the relaxation mechanism (Venu et al., 1999). Several types of MRI studies imply magnetization transfer from the solid lattice molecules to water in tissues (Navon et al., 2001; Neufeld et al., 2003); due to the complexity of the system, it has however been difficult to analyze the exchange processes in a site-resolved manner.

Over the last few years, magic-angle spinning (MAS) solid-state NMR (SSNMR) has emerged as a complementary tool to X-ray crystallography and solution NMR for the structural characterization of biomolecules. Remarkable advances in spectrometer hardware, sample preparation, as well as methodological developments, have recently allowed the sequential resonance assignments of several model proteins in the solid-state (Pauli et al., 2001; Böckmann et al., 2003; Igumenova et al., 2004a,b; Marulanda et al., 2004), as well as the first structure determination of a micro-crystalline protein (Castellani et al., 2002).

The recent use of deuterated proteins has allowed the study of the interactions between water and biomolecules in the solid state (Lesage and Böckmann, 2003; Paulson et al., 2003a). Deuteration for SSNMR studies was initially motivated by the reduction of the strong ^1H–^1H dipolar couplings in the sample (McDermott et al., 1992), as well as the possibility of distance measurements between re-exchanged amide protons in proteins (Reif et al., 2001; Reif et al., 2003) or carbon spins near selectively re-protonated sites (Morcombe et al., 2004). Unexpectedly, deuteration has also allowed unambiguous identification of interactions between water and proteins in the micro-crystalline state (Lesage and Böckmann, 2003; Paulson et al., 2003a). Indeed, while in protonated proteins Hα resonances are often found near or at the water frequency, this problem does not exist for deuterated samples. Thus, in 2D proton–carbon or proton–nitrogen correlation spectra, one can observe at the water frequency in the indirect dimension unambiguous water–protein cross signals. In analogy to proteins in solution, several mechanisms could be at the origin of the observed cross peaks, such as chemical exchange between a labile protein proton and a water proton, exchange relayed magnetization transfer, direct dipolar contacts between the water molecules and the protein, or, as proposed for micro-crystalline Ubiquitin (Paulson et al., 2003a), intermolecular nOe.

We have recently reported the observation of chemical exchange signals in ^1H–^{13}C CP-MAS HETCOR spectra of the micro-crystalline protein Crh (Lesage and Böckmann, 2003). Indeed, all cross signals observed belong to amino acids with exchangeable groups, like threonine, serine, tyrosine, and lysine. This shows that chemical exchange dominates water–protein magnetization transfer in this type of experiment in Crh. Still, other mechanisms can not be excluded and we currently investigate this more quantitatively in detail in a forthcoming contribution (manuscript in preparation). In the present paper, we concentrate on assignment strategies for water–protein interactions. We first consider the effects of deuteration on the NMR spectra of micro-crystalline Crh. We then perform a detailed analysis of the signals previously observed at the water frequency, in both ^1H–^{13}C and ^1H–^{15}N correlation spectra. In particular, by using a proton T_2'-selective ^1H–^{13}C–^{13}C correlation experiment, we are now able to provide site-specific assignments of the interacting residues. We compare the T_2' selective scheme to the observation of water–protein interactions at the water frequency. Finally, we correlate the observed exchange behavior of the serine and threonine hydroxyl protons, as well as lysine side chain amide protons, to structural features of the protein, particularly at the Crh dimer interface.

Materials and methods

Sample preparation

^{15}N, ^{13}C labeled Crh was prepared as described previously (Böckmann et al., 2003). ^{2}H, ^{13}C and ^{15}N-enriched Crh was prepared by growing bacteria in >98% ^{2}H, ^{13}C, ^{15}N labeled medium (Silantes). Exchangeable protons were re-exchanged under denaturing conditions (8 M Guanidinium Chloride). The proteins were renatured by tenfold dilution into 20 mM NH_4HCO_3 buffer, and were afterwards desalted. The protein was crystallized as described previously (Böckmann et al., 2003) by precipitation in the presence of 20% PEG 6000 in a crystallization plate over a 2 M NaCl solution. The precipitate resulting from about 8 mg of protein was centrifuged directly into a 4 mm CRAMPS rotor, and the rotor cap was sealed.

NMR experiments

All the spectra reported in this paper were recorded on a Bruker Avance spectrometer operating at a proton frequency of 500 MHz. The temperature of the sample was regulated at 267 K, corresponding to an actual sample temperature of about 5–10 °C, depending on the spinning speed. One-dimensional (1D) cross-polarization (CP) spectra and two-dimensional (2D) refocused INADEQUATE (Lesage et al., 1997) spectra were obtained using a 4 mm MAS ^{13}C–^{2}H–^{1}H triple resonance probe at a spinning frequency of 10 kHz. A 2 ms ramped CP (Metz et al., 1994) was used with radio-frequency (RF) fields of 56 and 83 kHz on the carbon and proton channels, respectively. SPINAL-64 proton decoupling (Fung et al., 2000) was applied during acquisition at a RF field of 66 kHz. When applied, deuterium decoupling was achieved using the Phase-Alternated Decoupling (PAD) sequence (Fu et al., 1996) at a decoupling power of 900 Hz and with intervals of 90 μs between the phase shifts. PAD ^{2}H decoupling was first optimized on a sample of 99.9% deuterated L-alanine (obtained from Sigma) where a reduction of the carbon linewidths of about 10 Hz could be observed (data not shown). For 2D refocused INADEQUATE spectra, an evolution period of 3.8 ms was used for the creation and re-conversion of double quantum coherences. Quadrature detection in t_1 was achieved using the TPPI method (Marion and Wüthrich, 1983). For the refocused INADEQUATE spectra on deuterated Crh, 300 t_1 increments were recorded with 256 scans each, yielding a total acquisition time in t_1 of 4.3 ms. On the protonated sample, 700 increments were recorded with 16 scans each. The other experimental parameters were the same as the ones used for the 1D spectra.

Two-dimensional ^{1}H–^{13}C and ^{1}H–^{15}N heteronuclear correlation (HETCOR) (van Rossum et al., 1997) spectra were recorded using a double resonance MAS probe at a spinning frequency of 12.5 kHz according to the pulse sequence described in detail elsewhere (Lesage and Böckmann, 2003). Homonuclear proton decoupling during t_1, was done using the DUMBO-1 decoupling scheme (Sakellariou et al., 2000) with a RF field of ~83 kHz. During t_2, the SPINAL-64 sequence (Fung et al., 2000) was applied at a decoupling power of 66 kHz. The recycle delay was set to 3 s. A X-channel 180° pulse was applied in the middle of the t_1 evolution time to refocus carbon–proton or nitrogen–proton scalar couplings, thereby improving the resolution in the proton dimension. In the ω_1 dimension, proton chemical shifts were corrected by applying a scaling factor of 0.46, as determined experimentally from a ^{1}H spectrum of L-Alanine recorded under similar conditions (Lesage et al., 2003). Proton and carbon chemical shifts were referenced externally to DSS (Markley et al., 1998). For the ^{1}H–^{13}C HETCOR experiment, 116 t_1 increments with 80 scans each were recorded. The total acquisition times in t_1 and t_2 were 8.12 and 10 ms respectively. A carbon π pulse of 7 μs was applied in the middle of the t_1 evolution period. A 2 ms ramped CP was used with 56 and 83 kHz on the carbon and proton channels, respectively. Quadrature detection in ω_1 was achieved using the States method (States et al., 1982). The ^{1}H–^{15}N HETCOR spectrum was recorded with similar parameters except for the number of scans, which was set to 160, and the nitrogen π pulse which was set to 8 μs.

The 1D T_2' selective spectra were acquired using 512 scans each and with dephasing times of 1, 2, 3, and 4 ms. Proton 90° pulses were 3 μs. A 2 ms ramped CP was used with 56 kHz on carbon and 83 kHz on the proton channel. Heteronuclear decoupling was achieved with SPINAL-64 at 66 kHz. The 2D T_2'-selective ^{1}H–^{13}C–^{13}C proton

driven spin diffusion (PDSD) spectrum was acquired with a dephasing time t_w of 1 ms. The mixing time was set to 20 ms. 1.2 ms were acquired in the indirect, and 15 ms in the direct dimension. Sixty-four increments were collected, with 512 scans, yielding a total acquisition time of 27 h. Pulse programs and phase cycles used here are available on our website (http://www.ens-lyon.fr/CHIMIE/Fr/Groupes/NMR) or upon request.

Results

Effects of deuteration on ^{13}C NMR spectra of micro-crystalline Crh

Figure 1a shows the one-dimensional carbon-13 spectrum of deuterated micro-crystalline Crh. For comparison, the 1D spectrum of the protonated form is shown in Figure 1c. It is obvious that the very high resolution observed for the protonated protein is not reproduced in the deuterated sample.

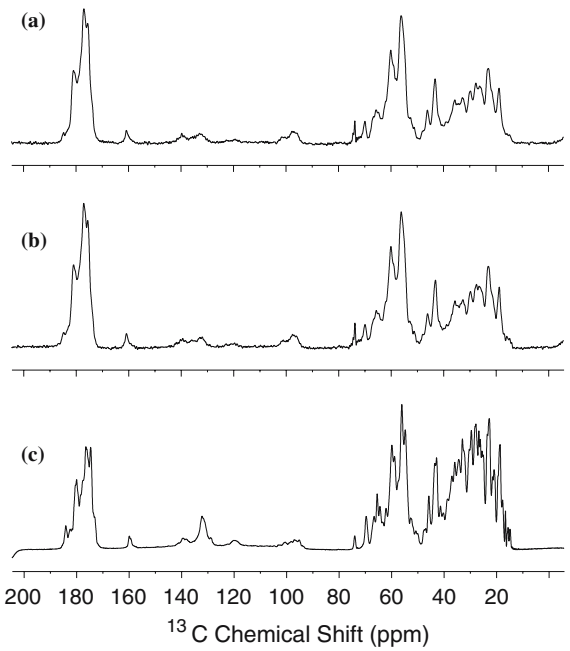

Figure 1. One-dimensional carbon-13 CP-MAS spectra of deuterated (a and b) and protonated (c) micro-crystalline Crh. In (b), ^2H decoupling was applied in addition to proton decoupling during acquisition. 1024 scans were accumulated with a recycle delay of 3 s. The ^{13}C signal to noise is weaker for the deuterated sample due to (i) a lower amount of protein in the rotor and (ii) the poor efficiency of the cross-polarization from the dilute bath of protons.

One possible origin for the observed broadening of the carbon resonances might be residual ^2H–^{13}C dipolar couplings (these couplings are however quite small, of the order of 500 Hz for a direct carbon–deuterium coupling, and are expected to be fully averaged out by the sample rotation) or, more likely, the ^2H–^{13}C scalar couplings (about 20 Hz for a sp^3 carbon). Deuterium decoupling was therefore applied, in addition to proton decoupling, during the acquisition of the carbon signal in order to suppress these two possible sources of broadening. The resulting 1D spectrum, obtained with PAD ^2H decoupling, is shown in Figure 1b. It does not exhibit significant improvement in terms of resolution compared to the proton-only decoupled ^{13}C spectrum (Figure 1a). Other ^2H decoupling schemes did not yield better resolution. This behavior is confirmed in Figure 2 which shows refocused INADEQUATE spectra of deuterated Crh acquired with (Figure 2b) or without (Figure 2a) ^2H decoupling applied during the whole length of the pulse sequence. As already observed in the 1D spectra, deuterium decoupling does not improve the resolution of the carbon resonances. Neither did increasing the proton decoupling power or the spinning frequency (up to 12 kHz) improve the ^{13}C lines.

Another possible source for ^{13}C line broadening could be residual protonation. Indeed, it is well-known from liquid-state NMR studies (Rosen et al., 1996) that deuterium isotope effects in partially deuterated samples lead to multiple carbon-13 resonances, which could induce line-broadening if not resolved. As demonstrated by heteronuclear correlation experiments (see below), the deuterated Crh sample is indeed not fully deuterated. In particular, residual protonation is observed for the methyl groups, which may correspond to CD_2H, CDH_2 or even CH_3 groups. It is difficult however to estimate the percentage of residual protonation, as no resolved lines are observed for the different species. To this end, quantitative comparison with the amino proton portion of the spectrum is also difficult, as two-bond transfers are involved in the observed NH-Cα cross peaks. The comparison of two-dimensional ^{13}C refocused INADEQUATE spectra recorded on the deuterated (Figure 2a) and protonated (Figure 2c) form show, however, that the carbon resonances are equally broadened in the fully deuterated Cα region (see below) and in

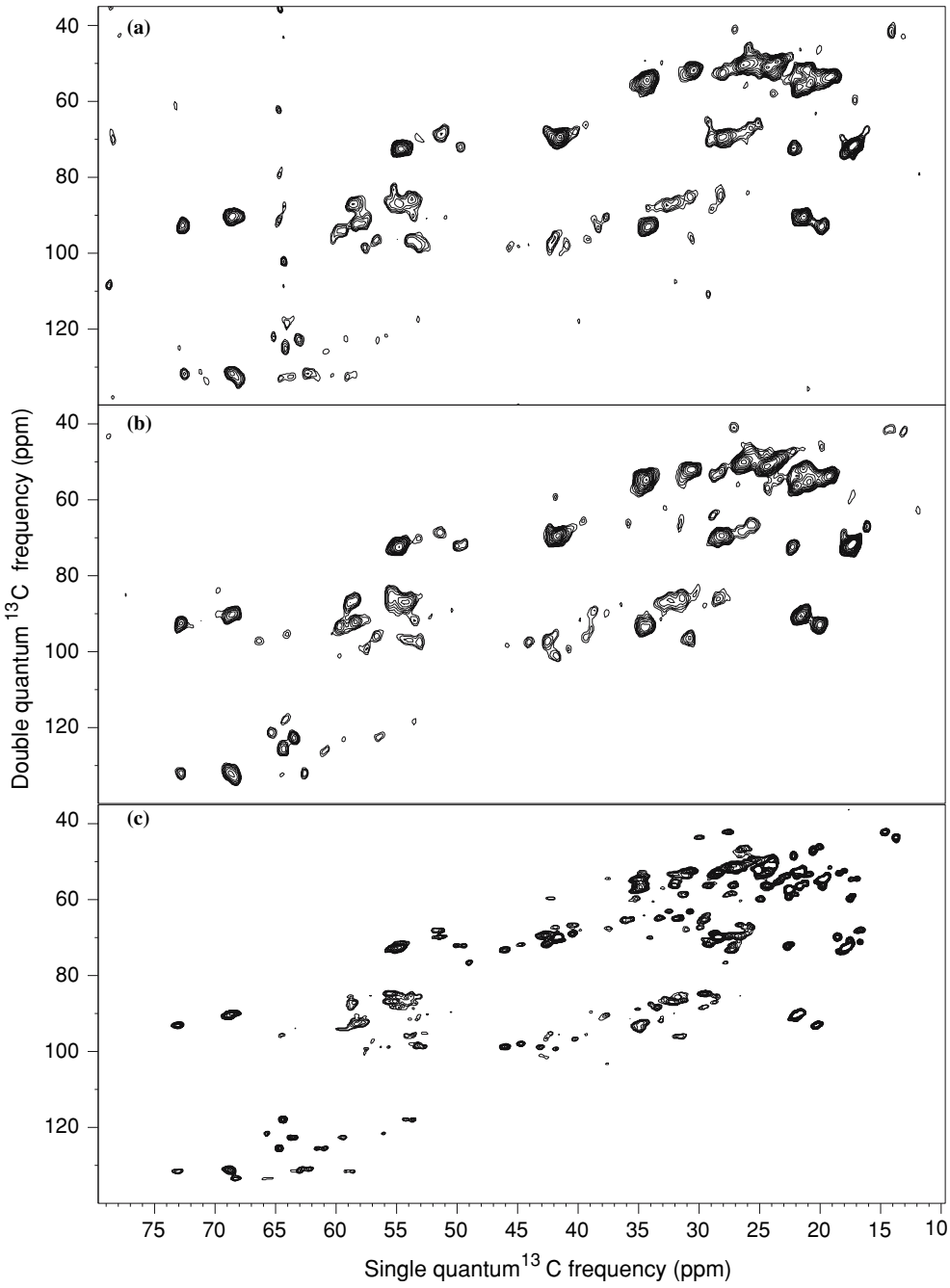

Figure 2. Two-dimensional carbon-13 refocused INADEQUATE spectra of deuterated (a and b) and protonated (c) micro-crystalline Crh. In (b), deuterium decoupling was applied in addition to proton decoupling after the CP step during the whole length of the pulse sequence.

the partially deuterated methyl region. The same observation is made for the carbonyl part of the 2D spectra (data not shown).

The data discussed above therefore suggest that, despite identical protocols for sample preparation, the relatively poor spectral resolution observed for deuterated Crh is the result of a slightly less ordered sample, yielding a larger distribution of chemical shifts for each individual carbon resonance. Finally, in analogy to the liquid

state, we observe shifts of the isotropic ^{13}C frequencies of about 0.3 ppm per directly attached ^{2}H, for the deuterated sites, and assignments of the deuterated carbons can thus be estimated from the assignments made on protonated Crh.

Effects of deuteration and temperature on ^{1}H spectra

The 1D proton spectrum of deuterated Crh, acquired after a single pulse, displays two narrow lines at 5.0 and 4.0 ppm (as referenced to external DSS, at a spinning speed of 10 kHz), which are assigned respectively to water and PEG 6000 (data not shown). The position of the water resonance is observed to shift to higher field with increasing MAS frequency. This effect is likely related to the temperature increase induced by the sample rotation at faster MAS rates. In liquid-state NMR (Cavanagh et al., 1996), the water chemical shift decreases with increasing temperatures, and the same temperature-chemical shift relationship holds here. The PEG resonance is not affected by spinning frequency, but seems to be dependent on sample preparation since it was observed at 3.8 ppm in the protonated sample, for which the PEG/water ratio is slightly higher than in the deuterated preparation (1 vs. 0.7 as measured from the integrated intensity of the proton resonances).

Residual protonation

Heteronuclear correlation spectroscopy performed on deuterated Crh allows the qualitative investigation of residual protonation. The 2D ^{1}H–^{13}C and ^{1}H–^{15}N spectra are shown in Figure 3a and b, respectively. As expected, correlations involving the back-exchanged amide protons are clearly observed with the Cα carbons (Figure 3a) and with the amide nitrogens (Figure 3b). In the ^{13}C dimension, correlations with the carbonyl region are also observed (data not shown). The ^{13}C–^{1}H HETCOR spectrum displays in addition cross-peaks in the methyl region. Using the ^{13}C assignments reported recently for protonated Crh, and taking into account the isotope shift induced by deuteration (Rosen et al., 1996), correlations could be assigned for the Hδ1 protons of Ile 47, Ile 64 and the Hε protons of Met 48, Met 51, as well as to overlapping Ala, Val and Leu methyl groups as reported in Figure 3a. This indicates that, despite the use of a $>98\%$ deuterated growth medium, a fraction of the methyl groups is partly protonated. Conversely, no signals are observed in the α proton chemical shift region, providing evidence for complete deuteration of these sites. Interestingly, a cross peak at 4.0 ppm in ω_1 and 72.4 ppm in ω_2 can be assigned to PEG, indicating that a fraction of this compound is sufficiently immobilized to

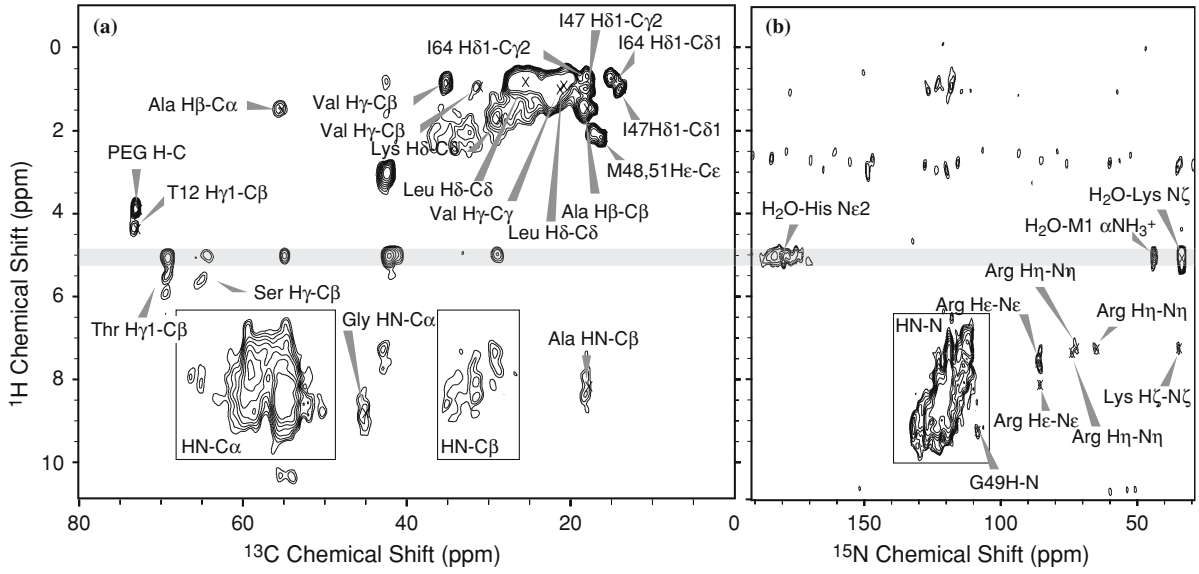

Figure 3. Two-dimensional ^{1}H–^{13}C (a) and ^{1}H–^{15}N (b) HETCOR spectra of deuterated micro-crystalline Crh. Cross-peaks were identified by analogy with the ^{13}C assignments reported for the protonated protein.(Böckmann et al., 2003).

yield cross-polarization. No interactions are however observed between the PEG and protein carbons in the HETCOR spectrum. In the ^{1}H–^{15}N correlation spectrum, in addition to backbone NH cross-peaks, we observe correlations for the back-exchanged Arg Hε and Hη side chain protons. Interestingly, in both heteronuclear correlation spectra, cross peaks are identified at the proton water frequency, which are described in more detail in the following.

Water–protein interactions

Some of the cross peaks observed at the water frequency in the 2D ^{1}H–^{13}C spectrum were previously assigned using chemical shift information of the protonated micro-crystalline form of Crh (Böckmann et al., 2003). Signals of Met 1 Cα, Glu 70 Cδ and Tyr 80 Cζ residues could be identified, as well as signals of Ser Cβ, Thr Cβ, His Cγ, Cδy, Cε1, and Lys Cε (Lesage and Böckmann, 2003). The latter could however not be site-specifically assigned using 2D spectra. As all these residues have labile protons known to display fast exchange rates in solution (Wüthrich, 1986), we concluded in our previous report that the cross-peaks at the water frequency arise most likely from chemical exchange with water on the millisecond time scale, and magnetization transfer to their neighboring ^{13}C spins during the CP step. In the ^{1}H–^{15}N HETCOR spectrum, correlations with water protons are also clearly observed. The (previously unassigned) αNH_3^+ nitrogen of the N-terminal Met1 is observed at 43.7 ppm in the ^{15}N dimension, and the side-chain Nε2 of the poly-His tag histidine residues at around 180 ppm. Most of the seven Lysine Nζ resonances at 35 ppm appear to be correlated with water protons; only a small εNH_3^+ signal is observed around a proton chemical shift of 7 ppm. In contrast, the Hη and Hε protons of the three arginine residues (Arg 9, 17, 28) do not show interactions with water. As in the ^{13}C-detected experiment, the correlations observed at the water frequency in the nitrogen-15 HETCOR spectrum very likely result from chemical exchange during the 2 ms spin-lock period between a water proton and a labile protein NH proton, which then transfers its magnetization to a nearby nitrogen nucleus by Hartmann–Hahn transfer. The backbone amide protons do not display any correlations with water molecules.

Ideally, in order to assign unambiguously the overlapping ^{13}C resonances that correlate with water protons, a three-dimensional experiment would be required in which, for example, a carbon mixing period would be added before direct detection. Such an approach was however not practicable in our hands on deuterated Crh within reasonable experimental time. In order to perform a site-specific assignment of residues interacting with water, we therefore employed the pulse sequence depicted in Figure 4a. This experiment relies on the application of a proton T_2' filter inserted prior to the CP step. As already proposed in the past by Harbison and co-workers (Harbison et al., 1988), a $t_w - \pi - t_w$ echo period, with a t_w delay of the order of a millisecond, allows for the selection of proton magnetization having long refocused

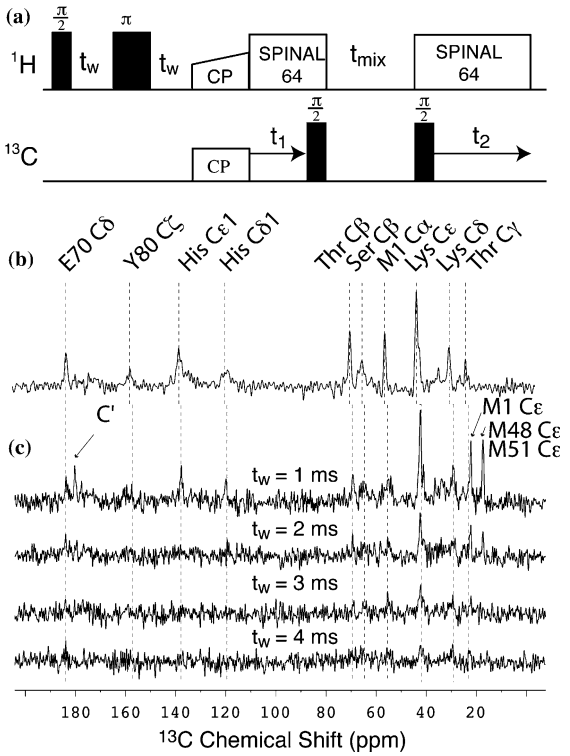

Figure 4. (a) Pulse sequence for the T_2' selective ^{1}H–^{13}C–^{13}C correlation experiment allowing the edition of residues interacting with water. (b) Carbon-13 trace extracted parallel to ω_2 at the water frequency in ω_1 from the 2D ^{1}H–^{13}C HETCOR spectrum of Figure 3a. (c) One-dimensional T_2' selective ^{1}H–^{13}C spectra of protonated Crh recorded using the pulse sequence shown in (a) for various lengths of the echo period, and with t_{mix} and t_1 set to zero. Arrows indicate signals observed in the selective spectra, but not in the 2D trace.

transverse relaxation times T_2', such as mobile water protons. In the absence of decoupling, the proton magnetization of the solid protein is expected to dephase much more rapidly, and should be mostly eliminated by the T_2' filter. The protons with long T_2' then transfer their magnetization to neighboring carbons through a CP step, followed by t_1 and a conventional proton-driven spin diffusion mixing time. The resulting (asymetric) spectrum is expected to selectively retain only correlations from carbons having fast exchangeable protons nearby, thereby providing site-specific identification of these atoms.

Figure 4c shows the 1D water selective spectra obtained for various values of the echo time t_w, and in Figure 4b for comparison the trace extracted at the water frequency along ω_2 from the 2D ^{1}H–^{13}C HETCOR spectrum of Figure 3a. It can be seen that the selective experiment effectively retains, as expected, all carbon resonances giving cross peaks with water in the HETCOR spectrum. Only few additional peaks are observed, pointed out by arrows in Figure 4c, and which correspond to Cε resonances of Met 48, 51 and likely of Met 1 (previously unassigned). Methionine Hε protons are assumed to have longer transverse dephasing times than other protein protons due to fast methyl group rotation in addition to the absence of other direct neighboring proton spins. An additional signal can also be observed in the carbonyl region. Thus, care has to be taken in interpreting the observed signals, and double checking with frequency-edited spectra is recommended.

The clear advantage of this type of experiment is that, due to selection by T_2' rather than by chemical shift, α-protons do not present a problem in this type of experiment, and the protonated Crh sample, with its higher S/N and better resolution can be used. The protonated form also allows the use of a simple PDSD experiment for further magnetization transfer. Moreover, the observed signals can

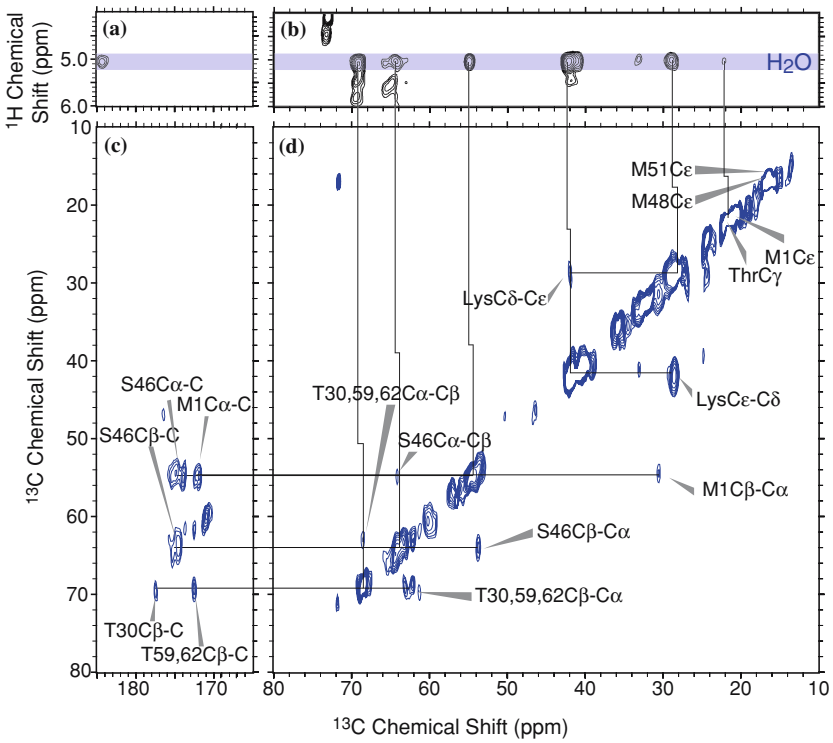

Figure 5. (a) and (b) are extracts around the water frequency in ω_1 from the 2D ^{1}H–^{13}C HETCOR spectrum of deuterated Crh shown in Figure 3a. (c) and (d) show the two-dimensional T_2' selective ^{1}H–^{13}C–^{13}C correlation spectrum recorded on protonated Crh for the carbonyl and aliphatic regions, respectively. Horizontal lines connect intra-residue correlations. Vertical lines connect resonances corresponding to the same carbon spin in the deuterated and protonated form. Note that the carbon-13 resonances in the deuterated protein (panels a and b) are shifted due to the deuterium isotope effect.

directly be identified using the previously reported ^{13}C chemical shift assignment of Crh.

Figure 5c and d show extracts in the carbonyl and aliphatic regions, respectively, of the T_2'-selective ^{1}H–^{13}C–^{13}C correlation spectrum recorded on protonated Crh. Extracts around the water frequency of the 2D HETCOR spectrum of Figure 3a (recorded on deuterated Crh) are displayed above for comparison (Figure 5a and b). Using the T_2' selective spectrum and the ^{13}C assignment previously reported for Crh (Böckmann et al., 2003), the site-specific assignment of many of the residues interacting with water can be established. The resonance at 68.5/63.0 ppm belongs to either or all Thr 30, 59 and 60 Cβ/Cα, which have nearly degenerate chemical shifts. The cross signal at 68.7/177.7 ppm in the carbonyl region allows however to clearly identify the Thr 30 Cβ/C resonance, and at 69.0/172.5 ppm either one or both Thr 59/62 Cβ/C resonances (which also have degenerate carbonyl chemical shifts). As to Thr 57, the present spectrum suggests through the absence of the corresponding Cα/Cβ cross signal that Thr 57 Hγ1 does not exchange with water on the observed time scale. The spectrum also confirms our previous observation that Thr 12, easily identified by its isolated Cβ resonance at 73.4 ppm, does not display any exchange cross peak with water. Thus among the five threonine residues present in Crh, only Thr 30 and one or both residues Thr 59 and 62 exhibit hydrogen exchange with water on the millisecond time scale.

Similarly, the cross-peak observed with water in the HETCOR spectrum at 64.2 ppm was previously tentatively assigned to correlations with Cβ resonances of residues Ser 46 and 52, which have almost degenerate chemical shifts at this frequency. However, the selective 2D experiment reveals that only Ser 46, identified by numerous intra-residue carbon-13 cross-signals (Cβ/Cα, Cα/Cβ, Cα/CO, and Cβ/CO), is interacting with water. No correlations are observed for residue Ser 52, as well as the two other serines, 31 and 56.

Although not residue-specific, the assignment of the lysine Cε resonances is confirmed in the 2D selective spectrum by the observation of Lys Cδ/Cε cross peaks at 28.6/41.7 ppm. The Met 1 Cα assignment could be cross-validated by studies of the Crh dimer interface (Etzkorn et al., 2004). In addition, cross peaks are observed at 55.0/30.9 and 54.8/171.9 ppm, which then can be assigned to Met 1 Cα/Cβ g and Cα/C′, respectively.

Several unassigned signals can be observed on the diagonal in the selective 2D spectrum in Figure 5d. They correspond to background protein signal due to uncomplete filtering, especially originating from protons in flexible parts of the protein, as for example the C-terminal region including the LQ6xHis extension. In particular, the C-terminal Val 85 Cα, Cβ chemical shifts, as well as the statistical His Cα, Cβ chemical shifts could explain most of the unassigned diagonal signals. However, 3D cross signals would be required for more specific assignments.

Dynamics of chemical exchange

Hydrogen exchange observed in HETCOR experiments between a labile protein proton and a water proton takes mainly place during the contact time of the cross-polarization step (a few milliseconds) and thus corresponds to residence times on the order of milliseconds. The proton resonances at the ω_1 water frequency are about 120 Hz wide, indicating that exchange affects the linewidths, as expected for the intermediate exchange regime. Magnetization buildup curves have been measured for CP times up to 4 ms, and reveal that magnetization build-up is still in the initial regime. Longer CP times would allow a more quantitative analysis of residence times, but were not attempted due to excessive sample heating on our system.

Discussion

Hydrogen exchange rates will clearly depend on some aspects of sample preparation. Water content in different protein crystals can vary about a broad range; water diffusion in a crystal can be more or less restricted. Narrow water resonances have not been observed in all micro-crystalline proteins (Chevelkov et al., 2003). The Crh microcrystals have a very high water content of about 67%, and the crystal packing results in high solvent permeability in all three dimensions (Juy et al., 2003). Also, pH does significantly affect exchange rates of nearly all exchangeable protons. Neutral pH, as used here for Crh, is interesting since close to physiological conditions, but is unusual in

NMR studies due to problems linked to fast amide proton exchange.

For proteins in solution, chemical exchange with water is an indicator for solvent accessibility and implication in hydrogen bonding. The residue specific assignment of the Thr and Ser residues in Crh, together with the known crystal structure of the Crh dimer (Juy et al., 2003), allows us to investigate this correlation in solid proteins. Figure 6 reports the location of all Ser and Thr residues on the crystal structure. In blue are shown those which show cross signals with water, and in pink those which are not observed at the water frequency. At least two out of five threonines yielded protein–water cross peaks: Thr 30 and 59 and/or 62. These threonines are located at the surface of the protein, and their hydroxyl protons do either not show any hydrogen bonds (Thr 62), or are hydrogen bonded to surface water (Thr 30), as observed in the crystal structure (Juy et al.,

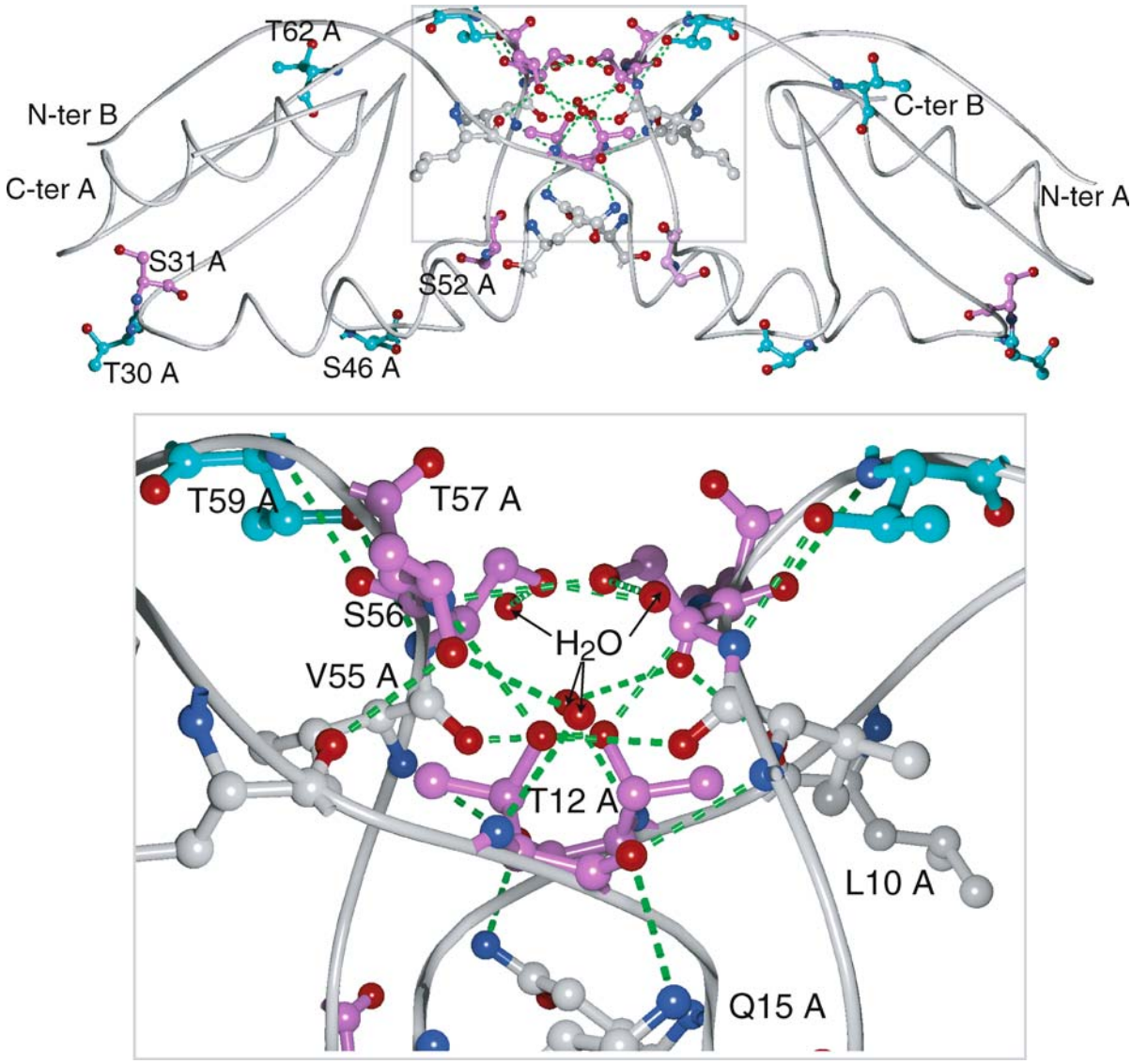

Figure 6. Serine and threonine residues with fast exchanging (blue) and slow exchanging (purple) hydroxyl protons illustrated on the 3D Crh dimer structure (PDB entry 1mu4 (Juy et al., 2003)). Labels are indicated for chain A only. Structures were drawn using Swiss-PDBViewer (Guex and Peitsch, 1997) and rendered with POV-Ray™.

2003). Thr 59 Oγ1 receives a hydrogen bond from Ser 56 HN, but its hydroxyl proton is not the donor. The hydroxyl proton of active site Ser 46 is also observed in the water selective spectra, and is also hydrogen-bonded to a surface water molecule.

The Ser 31 hydroxyl proton, which does not show fast exchange with water, is in fact not surface accessible, and is stabilized by an intramolecular hydrogen bond with the Asp 69 sidechain. In contrast, Ser 52, which does not show an exchange signal, is surface accessible, and no hydrogen bond is detected in the crystal structure. However, molecular dynamics simulations using the YASARA software (http://www.yasara.org) and the Amber99 force field (Wang et al., 2000) show that a hydrogen bond to Gly 49 CO is possible in a less static structure, which could explain our observations. The YASARA software was also used for a detailed analysis of the hydrogen bonds involving residues Thr 12, Ser 56 and Thr 57. Hydrogens were added to the crystal structure, the structure was minimized, and the hydrogen bonds were analyzed during a 300 μs trajectory. The residues Thr 12, Thr 57 and Ser 56, all of which do not show exchange signals, are indeed involved in an extensive hydrogen bonding network. The insert in Figure 6 shows in detail the network of hydrogen bonds to and from these residues, comprising intra- and intermolecular hydrogen bonds, involving residues from both monomers as well as four water molecules. Thr 12 Hγ1 donates a hydrogen bond to Val 55 C′, and accepts one from Thr 57 HN; Thr 57 Hγ1 donates a bond to Leu 10 C′, and accepts one from a water proton. Ser 56 Hγ donates a bond to a water molecule, and accepts one from Thr 59 HN. Extensive main chain hydrogen bonds involving these residues complement this large network involved in the stabilization of the Crh dimer interface.

The slow exchange of several hydroxyl protons is also indicated by the observation of resolved hydroxyl proton chemical shifts for several serine and tyrosine residues (Figure 3a). Thr12 Hγ1 resonates at 4.38 ppm, and signals are observed between 5 and 6 ppm at the Cβ chemical shift of the remaining Thr and Ser residues. All these resonances are shifted downfield with respect to the statistical Ser and Thr hydroxyl resonances (as reported in the BMRB), as expected for hydroxyl protons involved in hydrogen bonds (Berglund and Vaughan, 1980).

Doubling of resonances has been observed in some Crh spectra for several residues, including Thr 12, indicating local static or dynamic disorder (Böckmann et al., 2003). Our data indicate however that this seems not to compromise the implication of Thr 12 in the hydrogen bonding network observed in the crystal structure, as revealed by its hydroxyl proton chemical shift distinct from bulk water, as well as the absence of an exchange signal.

Hydroxyl exchange in solution has been thoroughly investigated by Otting and coworkers (Liepinsh et al., 1992; Liepinsh and Otting, 1996). Rates around 100 s^{-1} have been observed for free threonine hydroxyl groups at pH 7 and 10 °C (Liepinsh and Otting, 1996); for proteins, a wider range of exchange rates has been observed (50–200 s^{-1}, at pH 7 and 4 °C) (Liepinsh et al., 1992), mainly as a function of solvent accessibility. No correlation between hydroxyl exchange and involvement in hydrogen bonding could however be found there for the protein under study (BPTI). The relatively slow exchange rates observed here for the hydrogen bonded hydroxyl protons in Crh could be due to the extensive hydrogen bonding network found in Crh at the dimer interface, which might be more strongly stabilizing than the isolated hydrogen bonds found for hydroxyl protons in BPTI.

The εNH_3^+ of lysine residues 5, 11, 37, 40, 41 and 76 are totally solvent accessible and not involved in hydrogen bonds. In contrast, the highly conserved Lys45 residue shows hydrogen bonds from its εNH_3^+ protons to carbonyl groups of Phe 29 and Ser 31 (Juy et al., 2003). These hydrogen bonds are also present in the homologous protein HPr (Jia et al., 1993). Lys 45 is the neighboring residue to the active site Ser 46, and probably plays a role in stabilizing the local conformation. Lys 45 is the only lysine residue whose side chain is not oriented towards the solvent, but is lying flat on the protein surface. Lys 45 would thus be a good candidate for the non-exchanging εNH_3^+ proton signal observed at 7 ppm. In solution, lysine εNH_3^+ exchange rates were determined to have an average frequency of about 600 s^{-1} at pH 7 and 10 °C (as extrapolated from measurements at 36 and 20 °C (Liepinsh and Otting, 1996)).

None of the side chain protons of the three arginine residues 9, 17, 28 shows fast exchange with water. Average exchange frequencies of about 100 s^{-1} have been measured, respectively, for sol-

vent accessible εNH and ηNH_2 protons in arginine in solution, at pH 7 and 10 °C (Liepinsh and Otting, 1996). Arginine hydrogen exchange in micro-crystalline Crh is probably slowed down by the implication of all three Arginine side chains in hydrogen bonds. Indeed, Arg 9 is stabilized by an intra-monomer hydrogen bond to Glu 7, and an inter-monomer hydrogen bond to Gln 82 side chains; Arg17 by an inter-dimer hydrogen bond to the Ser 52 carbonyl group, and Arg 28 by an intra-monomer hydrogen bond to the Glu 25 side chain.

In the preceding discussion, we have focused on the effect of the molecular environment on hydrogen exchange. At given temperature and pH, exchange rates can in addition be modulated by the presence of exchange catalysts, or positive or negative charges at the protein. We do not consider these effects here, as they are more difficult to estimate (Liepinsh and Otting, 1996); however, such possible influences on the observed exchange rates can not be excluded.

Our observations indicate that protein surface accessibility for water in micro-crystalline Crh seems to be comparable to that expected in solution; for solvent exposed hydroxyl or amino protons, we observe exchange rates on the same order of magnitude as in solution. Most interestingly, in contrast to proteins in solution, exchange rates seem to be more significantly reduced if structural constraints, such as hydrogen bonds or partial burying, are present. This has also been observed for slowly exchanging amide protons in crystals of Lysozyme (Bentley et al., 1983; Pedersen et al., 1991) and BPTI (Gallagher et al., 1992), and was explained by damped motion in crystalline proteins compared to proteins in solution. Indeed, the spectrum of fluctuations giving rise to hydrogen exchange of less accessible or more stabilized protons might be significantly altered by the intermolecular interactions present within the crystalline state.

Finally, regarding the effects of deuteration, as solid state NMR on micro-crystalline proteins advances and more different protein samples are studied, it is becoming possible to distinguish general principles from protein-specific features. For example, no protein resonance line broadening has been reported for the two other deuterated proteins studied up to date (Reif et al., 2003; Morcombe et al., 2004). However, size, crystal packing, completeness of deuteration and pH are far from being the same for the different protein samples. Moreover, the higher size of the deuterons compared to protons, as well as the increased hydrophobicity induced by deuteration, can have a destabilizing effect on the complex structure of the domain swapped Crh dimer, notably at the dimer interface. Even, if little is known today about reproducibility of sample preparation, for Crh, most micro-crystalline preparations show comparable linewidths, with some few noteworthy exceptions including the deuterated samples considered here. Differences in resolution for virtually the same sample preparation procedures have also been reported in the literature (Paulson et al., 2003b).

Conclusion

Observation of hydrogen exchange is possible in micro-crystalline protein samples by solid state NMR techniques. Deuteration has been shown to allow the unambiguous observation of protein–water interactions, but is not without side effects on the quality of the protein spectra, at least in Crh. Proton T_2' selective carbon edited correlation spectra allow the use of protonated proteins, as well as the faster acquisition of higher-dimensional spectra. However, additional information is needed to discard cross signals arising from protein protons with long T_2'.

Exchange rates for surface accessible, non hydrogen bonded hydroxyl and amino protons seem to be comparable to proteins in solution. However, exchange seems to be more efficiently damped by hydrogen bonding or reduced surface accessibility in the crystal than in solution. Solid state NMR hydrogen exchange studies of additional proteins should allow to establish a more general picture in future.

Acknowledgements

This work was funded by CNRS and the French research ministry (ACI Biologie Cellulaire Moléculaire et Structurale 2003). Scientific discussions with Dr. S. Hediger and Dr. G. DePaëpe are gratefully acknowledged.

References

Bentley, G., Delepierre, M., Dobson, C., Wedin, R., Mason, S. and Poulsen, F. (1983) *J. Mol. Biol.*, **170**, 243–247.

Berglund, B. and Vaughan, R.W. (1980) *J. Chem. Phys.*, **73**, 2037–2043.

Böckmann, A. and Guittet, E. (1997) *FEBS Lett.*, **418**, 127–130.

Böckmann, A., Lange, A., Galinier, A., Luca, S., Giraud, N., Juy, M., Heise, H., Montserret, R., Penin, F. and Baldus, M. (2003) *J. Biomol. NMR*, **27**, 323–339.

Böckmann, A., Penin, F. and Guittet, E. (1996) *FEBS Lett.*, **383**, 191–195.

Buck, M., Radford, S. and Dobson, C.M. (1994) *J. Mol. Biol.*, **237**, 247–254 .

Castellani, F., van Rossum, B., Diehl, A., Schubert, M., Rehbein, K. and Oschkinat, H. (2002) *Nature*, **420**, 98–102.

Cavanagh, J., Fairbrother, W.J., Palmer, A.G. III and Skelton, N.J. (1996) *Protein NMR Spectroscopy: Principles and Practice*, Elsevier Science, USA.

Chevelkov, V., van Rossum, B.J., Castellani, F., Rehbein, K., Diehl, A., Hohwy, M., Steuernagel, S., Engelke, F., Oschkinat, H. and Reif, B. (2003) *J. Am. Chem. Soc.*, **125**, 7788–7789.

Dobson, C.M., Lian, L.-Y., Redfield, C. and Topping, K.D. (1986) *J. Magn. Reson.*, **69**, 201–209.

Etzkorn, M., Böckmann, A., Lange, A. and Baldus, M. (2004) *J. Am. Chem. Soc.*, **126**, 14746–14751.

Fu, R., Caldarelli, S., Ermakov, V. and Bodenhausen, G. (1996) *Solid State Nucl. Magn. Reson.*, **5**, 273–291.

Fung, B.M., Khitrin, A.K. and Ermolaev, K. (2000) *J. Magn. Reson.*, **142**, 97–101.

Gallagher, W., Tao, F. and Woodward, C. (1992) *Biochemistry*, **31**, 4673–4680.

Guex, N. and Peitsch, M.C. (1997) *Electrophoresis*, **18**, 2714–2723.

Harbison, G.S., Roberts, J.E., Herzfeld, J. and Griffin, R.G. (1988) *J. Am. Chem. Soc.*, **110**, 7221–7223.

Hwang, T.-L., Zijl, P.C.M.V. and Mori, S. (1998) *J. Biomol. NMR*, 221–226.

Igumenova, T.I., McDermott, A.E., Zilm, K.W., Martin, R.W., Paulson, E.K. and Wand, A.J. (2004a) *J. Am. Chem. Soc.*, **126**, 6720–6727.

Igumenova, T.I., Wand, A.J. and McDermott, A.E. (2004b) *J. Am. Chem. Soc.*, **126**, 5323–5331.

Jia, Z., Quail, J.W., Waygood, E.B. and Delbaere, L.T. (1993) *J. Biol. Chem.*, **268**, 22490–22501.

Juy, M., Penin, F., Favier, A., Galinier, A., Montserret, R., Haser, R., Deutscher, J. and Böckmann, A. (2003) *J. Mol. Biol.*, **332**, 767–776.

Krishna, M., Hoang, L., Lin, Y. and Englander, S. (2004) *Methods*, **34**, 51–64.

Lesage, A., Auger, C., Caldarelli, S. and Emsley, L. (1997) *J. Am. Chem. Soc.*, **119**, 7867–7868.

Lesage, A. and Böckmann, A. (2003) *J. Am. Chem. Soc.*, **125**, 13336–13337.

Lesage, A., Sakellariou, D., Hediger, S., Elena, B., Charmont, P., Steuernagel, S. and Emsley, L. (2003) *J. Magn. Reson.*, **163**, 105–113.

Liepinsh, E. and Otting, G. (1996) *Magn. Reson. Med.*, **35**, 30–42.

Liepinsh, E., Otting, G. and Wüthrich, K. (1992) *J. Biomol. NMR*, **2**, 447–465.

Marion, D. and Wüthrich, K. (1983) *Biochem. Biophy. Res. Com.*, **113**, 967–974.

Markley, J.L., Bax, A., Arata, Y., Hilbers, C.W., Kaptein, R., Sykes, B.D., Wright, P.E. and Wüthrich, K. (1998) *Eur. J. Biochem.*, **256**, 1–15.

Marulanda, D., Tasayco, M.L., McDermott, A., Cataldi, M., Arriaran, V. and Polenova, T. (2004) *J. Am. Chem. Soc.*, **126**, 16608–16620.

McDermott, A.E., Creuzet, F.J., Kolbert, A.C. and Griffin, R.G. (1992) *J. Magn. Reson.*, **98**, 408–413.

Metz, G., Wu, X.L. and Smith, S.O. (1994) *J. Magn. Reson. Ser. A*, **110**, 219–227.

Morcombe, C.R., Gaponenko, V., Byrd, R.A. and Zilm, K.W. (2004) *J. Am. Chem. Soc.*, **126**, 7196–7197.

Mori, S., Abeygunawardana, C., van Zijl, P.C.M. and Berg, J.M. (1996) *J. Magn. Reson. B*, **110**, 96–101.

Navon, G., Shinar, H., Eliav, U. and Seo, Y. (2001) *NMR Biomed.*, **14**, 112–132.

Neufeld, A., Eliav, U. and Navon, G. (2003) *Magn. Reson. Med.*, **50**, 229–234.

Pauli, J., Baldus, M., van Rossum, B., de Groot, H. and Oschkinat, H. (2001) *Chembiochem.*, **2**, 272–281.

Paulson, E.K., Morcombe, C.R., Gaponenko, V., Dancheck, B., Byrd, R.A. and Zilm, K.W. (2003a) *J. Am. Chem. Soc.*, **125**, 14222–14223.

Paulson, E.K., Morcombe, C.R., Gaponenko, V., Dancheck, B., Byrd, R.A. and Zilm, K.W. (2003b) *J. Am. Chem. Soc.*, **125**, 15831–15836.

Pedersen, T., Sigurskjold, B., Andersen, K., Kjaer, M., Poulsen, F., Dobson, C. and Redfield, C. (1991) *J. Mol. Biol.*, **218**, 413–426.

Raschke, T.M. and Marqusee, S. (1998) *Curr. Opin. Biotechnol.*, **9**, 80–86.

Reif, B., Jaroniec, C.P., Rienstra, C.M., Hohwy, M. and Griffin, R.G. (2001) *J. Magn. Reson.*, **151**, 320–327.

Reif, B., Van Rossum, B.J., Castellani, F., Rehbein, K., Diehl, A. and Oschkinat, H. (2003) *J. Am. Chem. Soc.*, **125**, 1488–1489.

Rosen, M.K., Gardner, K.H., Willis, R.C., Parris, W.E., Pawson, T. and Kay, L.E. (1996) *J. Mol. Biol.*, **263**, 627–636.

Sakellariou, D., Lesage, A., Hodgkinson, P. and Emsley, L. (2000) *Chem. Phys. Lett.*, **319**, 253–260.

Spera, S., Ikura, M. and Bax, A. (1991) *J. Biomol. NMR*, **1**, 155–165.

States, D.J., Haberkorn, R.A. and Ruben, D.J. (1982) *J. Magn. Reson.*, **48**, 286–292.

van Rossum, B.-J., Förster, H. and de Groot, H.J.M. (1997) *J. Magn. Reson.*, **124**, 516–519.

van Zijl, P.C., Zhou, J., Mori, N., Payen, J.F., Wilson, D. and Mori, S. (2003) *Magn. Reson. Med.*, **49**, 440–449.

Venu, K., Svensson, L.A. and Halle, B. (1999) *Biophys. J.*, **77**, 1074–1085.

Wang, J., Cieplak, P. and Kollman, P. (2000) *J. Comput. Chem.*, **21**, 1049–1074.

Wüthrich, K. (1986) *NMR of Proteins and Nucleic Acids* Wiley, New York, NY.